Redox Biology 69 (2024) 103017

Contents lists available at ScienceDirect

Redox Biology

journal homepage: www.elsevier.com/locate/redox

Flavonoid 4,4′-dimethoxychalcone selectively eliminates senescent cells via activating ferritinophagy

Tianxiang Wang [1], Changmei Yang [1], Zhiqiang Li, Ting Li, Ran Zhang, Yujiao Zhao, Tianyi Cheng, Zhaoyun Zong, Yingying Ma, Dongyuan Zhang, Haiteng Deng [*]

MOE Key Laboratory of Bioinformatics, Center for Synthetic and Systematic Biology, School of Life Sciences, Tsinghua University, Beijing, 100084, PR China

ARTICLE INFO

Keywords:
4,4′-dimethoxychalcone
Senescence
Senolytics
Ferroptosis
FECH
Ferritinophagy

ABSTRACT

Flavonoids are bioactive natural polyphenolic compounds with health benefits, including anti-tumor, anti-inflammatory and anti-aging effects. Our previous studies revealed that a flavonoid 4,4′-dimethoxychalcone (DMC) induced ferroptosis via inhibiting ferrochelatase (FECH). However, the effect of DMC on cellular senescence is unknown. In the present study, we found that DMC treatment selectively eliminated senescent cells, and DMC alone or a combination of DMC and quercetin or dasatinib showed high efficiency in the clearance of senescent cells. We identified FECH was highly expressed in senescent cells compared to non-senescent cells. Mechanistically, we found that DMC inhibited FECH and induced ferritinophagy, which led to an increase of labile iron pool, triggering ferroptosis of senescent cells. Importantly, we found that DMC treatment prevented hair loss, improved motor coordination, and reduced the expression of several senescence-associated secretory phenotype factors (*IL-6*, *IL-1β*, *CXCL-10*, and *MMP12*) in the liver of old mice. Collectively, we revealed that, through the induction of ferroptosis, DMC holds the promise as a new senolytics to prevent age-related pathologies.

1. Introduction

Cellular senescence refers to a cellular state involving an irreversible cell cycle arrest, chromatin changes, apoptosis resistance and increased secretion of pro-inflammatory cytokines, chemokines, and extra-cellular matrix-degrading proteins, a feature termed as senescence-associated secretory phenotype (SASP), which underlies many age-related pathologies. A great number of studies have shown that senescent cells accumulate during ageing in multiple tissues [1]. Senescent cells and SASP cause a state of chronic inflammation, which drives many age-related diseases [2,3]. The elimination of senescent cells has been shown to alleviate the onset of several pathologies and increase mouse lifespan [4,5]. Tremendous efforts have thus been made to identify senolytic compounds to selectively eliminate senescent cells. The combination of dasatinib (D) and quercetin (Q) has been identified and used as senolytics, which efficiently induces apoptosis in senescent cells, and shows anti-aging effect in animals [4]. Now, the senolytics D + Q has moved forward to the stage of clinical trials [6].

Flavonoids are a group of secondary natural metabolites produced by plants with biological activities. Multiple studies have documented the anti-oxidative, anti-aging, anti-inflammatory, and anti-tumor effects of flavonoids [7]. In addition, flavonoids, including quercetin [4], fisetin [8] and procyanidin C1 [9], also have senolytic properties. The flavonoid 4,4′-dimethoxychalcone (DMC) is particularly abundant in the plant *Angelica keiskei koidzumi*, which has been used in Asian traditional medicine, and was documented for its ability to promote autophagy-dependent longevity and health [10]. Previously, we investigated the targets of DMC via thermal proteome profiling (TPP) and found that DMC synergistically inhibited ferrochelatase (FECH) and activated Keap1/Nrf2/HMOX1 pathway to induce ferroptosis in cancer cells [11,12]. FECH is a metalloenzyme catalyzing the final step of heme biosynthesis, the insertion of ferrous iron into protoporphyrin IX (PPIX) to produce heme [13]. By inhibiting the enzymatic activity of FECH, DMC induces iron accumulation and further ferroptosis [12].

Ferroptosis is an iron-dependent form of cell death that is triggered by lipid peroxidation [14]. Morphologically, cells undergoing ferroptosis exhibit reduced numbers of mitochondrial cristae and shrunken mitochondria [14,15]. Cytoplasmic iron is mainly stored in ferritin and can be released under periods of iron demand [16]. Nuclear receptor coactivator 4 (NCOA4) mediated ferritinophagy enables the degradation of ferritin, which increases the level of cytoplasmic labile iron pool to

* Corresponding author. School of Life Sciences, Tsinghua University, Haidian, Beijing, 100084, PR China.
E-mail address: dht@mail.tsinghua.edu.cn (H. Deng).
[1] These authors contributed equally.

https://doi.org/10.1016/j.redox.2023.103017
Received 3 November 2023; Received in revised form 26 December 2023; Accepted 27 December 2023
Available online 30 December 2023

Abbreviations

SASP	senescence-associated secretory phenotype
DMC	4,4′-dimethoxychalcone
FECH	ferrochelatase
D	dasatinib
Q	quercetin
TPP	thermal proteome profiling
CQ	chloroquine
PPIX	protoporphyrin IX
POR	NADPH-cytochrome P450 reductase
MDA	malondialdehyde
LPCAT3	lysophosphatidylcholine acyltransferase 3
ALOX5	arachidonate 5-lipoxygenase

induce ferroptosis [17]. Previous studies have shown that senescent cells have impaired ferritinophagy and inhibited ferroptosis [18]. However, ferroptosis, as one of the modes of inflammatory-related cell death, also has been reported that it can be increasingly activated by alterations in cellular function and metabolism during aging [19]. Thus, the mechanism of ferroptosis in senescent cells is unknown, and it is not clear that DMC can induce ferroptosis in senescent cells as well as have senolytic effects.

In this study, using a vicarious and unbiased bioinformatics method, we demonstrated that ferroptosis was inhibited in senescent cells compared with control cells and the ability of DMC to induce ferroptosis of senescent cells. We demonstrated that DMC induced ferroptosis and selectively eliminated senescent cells *in vitro*. DMC induced ferritinophagy which along with FECH inhibition, led to an increase of labile iron pool and triggered ferroptosis in senescent cells. Then, we found that DMC or DMC + Q treatment significantly reduced senescent cell number and SASP in mouse liver tissues. Importantly, DMC treatment showed low toxicity and improved physical functions in old mice. In summary, our study reported for the first time that DMC, a flavonoid, functions as a senolytic by inducing ferroptosis in senescent cells.

2. Materials and methods

2.1. Cell preparation and culture, reagents

LO2 cells and 293 T cells (purchased from the cell bank of the Chinese Academy of Sciences), primary mouse fibroblasts (isolated from 7-month-old mouse tail) were cultured in DMEM (Wisent, Montreal, Canada). The culture medium was supplemented with 10 % fetal bovine serum (FBS) (PAN-Biotech, Germany) and 1 % penicillin/streptomycin (Wisent, Montreal, Canada). Human umbilical vein endothelial cells (HUVECs) (Guandao, China) were cultured in Endothelial Cell Medium (Sciencell, USA). Cells were cultured in a humidified incubator containing 5 % CO_2 at 37 °C.

DMC was purchased from Alfa Aesar (Cat# L10585, USA), quercetin (Cat# T2174) and Dasatinib (Cat# T1448) were purchased from TargetMol (USA), etoposide was purchased from Beyotime (Cat# SC0173, China), Ferrostatin-1 was purchased from Aladdin (Cat# F129882, China).

2.2. Animal experiments

Mice experiments were performed in the animal facility of Tsinghua University (Beijing, China) with approval of the Institutional Animal Care and Use Committee of Tsinghua University (Approval number: 23-DHT3). C57BL/6 J WT mice was purchased from Jackson Laboratory through Laboratory Animal Research Center and housed in animal facility of Tsinghua University with ad libitum access to diet and water. Animal rooms were maintained at 20–22 °C with 30–70 % relative humidity and a 12-h light/dark cycle. DMC was dissolved in DMSO at 20 mg/mL and then was diluted to the working concentration. 20-month-old C57BL/6 J male mice were intraperitoneally injected with 50 mg/kg DMC or 25 mg/kg DMC +25 mg/kg quercetin every four or five days for 2 months.

2.3. Western blotting

Cells were lysed in RIPA lysis buffer (Cat# P0013K, Beyotime, China) added with Protease inhibitors cocktail. Equal volumes of proteins were separated by 12 % sodium dodecyl sulfate-polyacrylamide gel electrophoresis (SDS-PAGE) and electro-transferred onto a polyvinylidence difluoride (PVDF) membrane. Primary rabbit *anti*-FECH (Cloud-Clone, Wuhan, China), rabbit anti-Ferritin (Abcam, Cambridge, UK), rabbit *anti*-GPX4 (HuaBio, Hangzhou, China), rabbit *anti*-p21-Waf1/Cip1 (Cell Signaling Technology, Danvers, USA), rabbit *anti*-p16-INK4A (Proteintech, Chicago, USA), rabbit *anti*-LC3 (Proteintech, Chicago, USA), rabbit *anti*-p62 (Cell Signaling Technology, Danvers, USA), rabbit anti-actin (Cloud-Clone, Wuhan, China), and secondary anti-rabbit HRP-IgG antibodies (Cell Signaling Technology, Danvers, USA) were used for immunoblotting.

2.4. Sample preparation for tandem mass tag (TMT) quantitative proteomic analysis

Three groups of cells, including the control LO2 group, the senescent LO2 group, and the 50 μM DMC-treated senescent LO2 for 48 h group (SD), were lysed by RIPA lysis buffer (Cat# P0013K, Beyotime, China) added with Protease inhibitors cocktail, and the supernatant was added to acetone in a 1:5 vol at −30 °C for precipitation and dissolved with 8 M urea. Take 150 μg of protein per sample and digest with trypsin at 37 °C overnight for 16 h. Tryptic peptides were desalted and labeled with the TMT 9-plex reagents (Thermo Scientific, Cat# 90110). Then, the mixed labeled peptides were subjected to LC-MS/MS analysis.

2.5. LC-MS/MS analysis and protein identification and quantification

LC-MS/MS analysis was performed as described previously [11]. Labeled peptides were injected onto a UHPLC 3000 system coupled to a Thermo Scientific Orbitrap Exploris™ 480 mass spectrometer using a C-18 analytical column (300 Å, 5 μm, Thermo Fisher Scientific, USA). The peptides were eluted with a gradient elution program at a flow rate of 0.300 μL/min. Mobile phase A consisted of 0.1 % formic acid, and mobile phase B consisted of 100 % acetonitrile and 0.1 % formic acid. The mass spectrometer was operated in the data-dependent acquisition (DDA) mode using Xcalibur 4.5.445.18 software. MS1 spectra were acquired at a mass range of 300–1800 m/z with a resolution of 60,000. The spray voltage was set at 2100 V, and the Automatic Gain Control (AGC) target was set to $3e^6$. For MS2 scans, the top 40 most intense precursor ions were fragmented in the HCD collision cell at a normalized collision energy of 32 % using a 0.4 Da isolation window. The dynamic exclusion duration was set to 15 s, and the AGC target was set to $1e^5$ while the maximum injection time was set to 100 m.

The raw mass spectrometry data were searched against the Homo Sapiens database by the Proteome Discoverer 2.3 software. Raw data of LC-MS/MS have been uploaded to the iProx website (https://www.iprox.org). The accessible number is IPX0007606000.

2.6. Exploration of inflammatory cell death pathways for TMT quantitative proteomics based on bioinformatics

To explore and objectively assess the activity of the inflammatory cell death pathways between the three groups (Ctrl, SEN, SEN + DMC), gene sets downloaded from Molecular Signatures Database (MSigDB) (https://doi.org/10.1073/pnas.0506580102), including

WP_FERROPTOSIS.v2023.1. Hs.gmt, REACTOME_PYROPTOSIS. v2023.1. Hs.gmt, GOBP_NECROPTOTIC_SIGNALING_PATHWAY. v2023.1. Hs.gmt, HALLMARK_APOPTOSIS.v2023.1. Hs.gmt were applied to respectively evaluate activities of ferroptosis, apoptosis, pyroptosis and necroptosis based on Single-Sample Gene Set Enrichment Analysis (ssGSEA) via the GSVAR package. The results of TMT quantitative proteomics are shown in Supplementary Table 1. Detailed genes and pathway scores are shown in Supplementary Table 2 and Supplementary Table 3, respectively. After normalizing the scoring, the difference in inflammatory cell death pathways between groups was exhibited by the Heatmap R package.

2.7. Transmission electron microscopy (TEM)

Ultrastructural morphology of the cells was examined by transmission electron microscopy (TEM). The method was described as previously [12]. Briefly, cells were cultured in a 3.5 cm cell culture dish and subsequently fixed using an electron microscope fixing solution for 2–4 h. The fixed cells were then embedded in 1 % agarose, dehydrated, and cut into ultrathin sections (60–80 nm) using an ultramicrotome (Leica UC7, Leica). Sections were stained with uranyl acetate in pure ethanol for 15 min, followed by staining with lead citrate for 15 min. Images were acquired with Transmission Electron Microscope (HT7700, HITACHI). At least 10 images were acquired and representative images are shown.

2.8. Malondialdehyde measurement

Malondialdehyde (MDA) levels were measured using MDA assay kit (Solarbio, China, Cat# BC0020) following the manufacturer's instructions. Briefly, cells collected in centrifuge tubes were disrupted with ultrasound to make 1 mL of extract per 5 million cells. Take the supernatant after centrifugation at 8000*g* for 10 min at 4 °C. After incubation with detection buffer at 100 °C for 1 h. The absorbance at 532 nm was measured in the supernatant with a spectrophotometer.

2.9. Intracellular total iron measurements

Intracellular total iron was measured using an Intracellular Iron Colorimetric Assay Kit (Cat# E1042, Applygen, China) following the manufacturer's instructions. Briefly, cells were collected and washed twice with PBS after drug treatment. Then cells were collected and lysed in lysis buffer. The lysate was mixed with 4.5 % potassium permanganate solution at 1:1 ratio. The mixture was incubated at 60 °C for 1 h. Then, after the addition of the iron ion detection reagent, the mixture was incubated at room temperature for 30 min, the absorbance at 550 nm in the sample was measured with a spectrophotometer. Intracellular iron level was normalized to protein concentration.

2.10. Cell viability assay

Cells were seeded and cultured in 96-well plates. After treatment, the cell survival rate was measured using CCK-8 reagent (Cat# K1018, ApexBio Technology, USA) according to the manufacturer's instructions. Briefly, CCK-8 reagent was added into the wells, then the plates were incubated in a cell incubator for 1.5 h. The absorbance at 450 nm was measured to calculate cell viability.

2.11. Cell apoptosis assay

Apoptosis assay was carried out by utilizing a FITC Annexin V Apoptosis Detection Kit (BD Biosciences, Cat# 556547) according to the manufacturer's instructions. Briefly, after treatment, cells were collected and washed twice with PBS and were resuspended in binding buffer. Then FITC Annexin V and Propidium Iodide (PI) were added and incubated in the dark at room temperature for 15 min. Finally, 10,000 cells were analyzed by using a BD Flow Cytometer (BD Biosciences, NJ, USA).

2.12. Real-time quantitative PCR analysis (RT-qPCR)

Total RNA was isolated from cells by using Trizol reagent (TIANGEN, Beijing, China). Liver tissues were added into Trizol reagent and homogenized with a grinding rod. Then cDNA was synthesized using a commercially available kit following the manufacturer's instructions (CWBIO, Beijing, China). qPCR analysis was performed using SYBR green reaction mixture (CWBIO, Beijing, China) and Roche LightCycler 96 System (Roche, Basel, Switzerland). β-Actin was used as internal control for relative quantification. Primers used in qPCR are listed in Supplementary Table 4.

2.13. Hematoxylin-eosin (HE) staining

Tissues were fixed with 4 % paraformaldehyde overnight. Then, tissues were embedded in paraffin. Then, 5 μm sections were prepared, deparaffinized and hydrated sequentially, stained with hematoxylin and eosin. The sections were then dehydrated by gradient alcohol, transparentized with xylene, then were mounted with neutral resin for light microscopy.

2.14. Immunohistochemistry (IHC) staining

Tissues were fixed with 4 % paraformaldehyde overnight. Then, tissues were embedded in paraffin according to the standard protocol. Then 5 μm sections were prepared, deparaffinized and hydrated sequentially. Antigen retrieval was performed using EDTA buffer (Servicebio), then endogenous peroxidase was blocked. Then slides were blocked with 3 % BSA at room temperature for 30 min, before incubation with primary antibody (IL-6/IL-1β, Servicebio) at 4 °C overnight. After being washed with PBS twice, slides were incubated with secondary antibody (Servicebio). Signal was detected by DAB staining. Nuclear was stained by hematoxylin. The sections were then dehydrated by gradient alcohol, transparentized with xylene, then were mounted with neutral resin for light microscopy.

2.15. SA-β-galactosidase staining

Cellular senescence was assessed by examining the activity of β-galactosidase using SA-β-Gal staining kit (Cat# C0602, Beyotime, China) according to the manufacturer's instructions. Briefly, the cells in 12-well plates were fixed with fixation solution for 10 min, then washed with PBS twice and stained with SA-β-Gal solution at 37 °C overnight. For SA-β-Gal activity in the liver tissues, 8 μm frozen sections were fixed with β-galactosidase staining fixation solution for 1 h, washed with PBS twice and were incubated with SA-β-Gal staining solution at 37 °C overnight. Then the samples were imaged by light microscopy (Nikon-90i, Japan), and the blue-stained cells were identified as senescent cells.

2.16. Rotarod test

Mice were trained on the Rotarod at a speed of 10 rpm for 3 days. During the test, the speed of the Rotarod was 10 rpm, and the time on the rod before falling was recorded.

2.17. siRNA knockdown of FECH in cells

Cells were grown in 6-well plates until 50 % confluency was achieved. TRANSFECTION reagent (4 μl, Signagen) mixed with 100 nM siRNA was added into each well according to the manufacturer's instructions. For *FECH* knockdown, 100 nM siRNA wase used, and for negative control, NC siRNA negative control was used. Cells were cultured for 48 h after transfection before harvest for experiments.

FECH siRNA:

Sense: GCUUAAAUGCCAUUUACAGtt.

Antisense: CUGUAAAUGGCAUUUAAGCtg.

NC siRNA:
Sense: UUCUCCGAACGUGUCACGUtt.
Antisense: ACGUGACACGUUCGGAGAAtt.

2.18. Statistical analysis

Student's *t*-test was used to compare two groups. And one-way ANOVA was used for multiple comparisons. $P < 0.05$ was considered statistically significant. Data were presented as the means ± SD. GraphPad Prism software (version 9.0) was used for statistical analysis.

3. Results

3.1. DMC and its combination with dasatinib or quercetin selectively eliminate senescent cells

In order to investigate whether DMC has the ability to clear senescent cells, we employed several senescent cell models using different cell lines. To generate replicative senescent cells, primary mouse fibroblasts were passaged for 8 times after isolation, and human umbilical vein endothelial cells (HUVECs) were passaged for 4 times. Additionally, we adopted a DNA damage-induced senescent cell model by treating LO2 cells (human normal hepatocytes) with 10 μM etoposide for 24 h. We treated senescent primary mouse fibroblasts, HUVECs and LO2 cells with DMC at increasing concentrations for 48 h, 12 h, and 48 h, respectively. SA-β-Gal staining results showed that senescent cells were eliminated in a dose-dependent manner (Fig. 1A–C). In addition, we treated the cells with DMC combined with dasatinib (D) or quercetin (Q). The results showed that both DMC + D and DMC + Q treatments remarkably reduced senescent cell numbers (Fig. 1A–C). Compared with D + Q, a lower concentration (300 nM + 10 μM) of D + DMC was required to achieve the same senescence cell-eliminating effect, which suggests that DMC was lower than Q when combined with D in eliminating senescent cells (Fig. 1A). SA-β-Gal staining results showed that

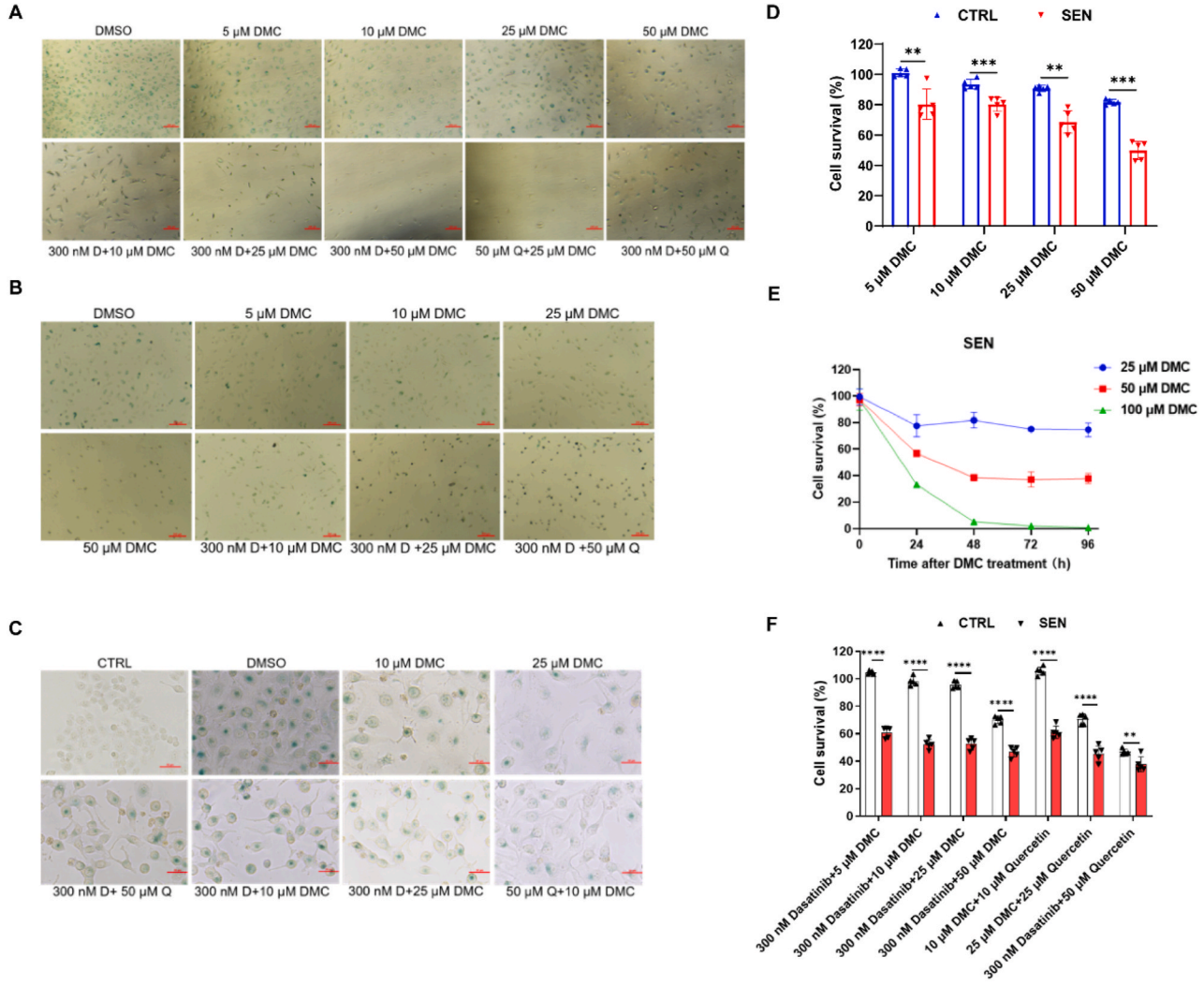

Fig. 1. DMC and its combination with dasatinib or qurcetin exhibit senolytic activity.
(A) SA-β-Gal staining results: Primary mouse fibroblasts were passaged for 8 passages to create a replicative senescent cell model, then treated with varying concentrations of DMC and its combination for 48 h. Scale bar: 200 μm. (B) SA-β-Gal staining results: Human umbilical vein endothelial cells (HUVECs) were passaged for 4 passages to establish a replicative senescent cell model, followed by treatment with different concentrations of DMC and its combination for 12 h. Scale bar: 200 μm. (C) SA-β-Gal staining results: LO2 cells were treated with 10 μM etoposide to induce DNA damage-induced senescence, then exposed to different concentrations of DMC and its combination for 48 h. Scale bar: 50 μm. (D) Cell survival assessment: Ctrl and senescent LO2 cells were seeded in 96-well plates, treated with DMSO or DMC for 48 h, and subjected to CCK-8 analysis (n = 5). (E) Cell survival assessment: Senescent LO2 cells were seeded in 96-well plates, treated with DMSO or DMC for 48 h, and subjected to CCK-8 analysis (n = 5). (F) Cell survival assessment: Ctrl and senescent LO2 cells were seeded in 96-well plates, treated with DMSO, DMC, Dasatinib, and quercetin for 48 h, followed by CCK-8 analysis (n = 5). D: Dasatinib, Q: quercetin. Ctrl: control cells. SEN: senescent cells. Data were analyzed using Student's *t*-test. ****p < 0.0001; ***p < 0.001; **p < 0.01; *p < 0.05. *p < 0.05 was considered statistically significant. All values represent the mean ± SD.

senescent LO2 cells were successfully generated by treating with etoposide (Fig. 1C). Quantitative PCR results showed that the expression levels of senescence-associated secretory phenotype (SASP) factors (*IL-1α*, *IL-1β*, *IL-6*, *IL-8*, *PAI-1*, *MCP1*, *MMP12*) were significantly increased in LO2 cells after etoposide treatment (Fig. S1A). Likewise, the mRNA levels of DNA damage factors *p21*, *p16* and *p53* were also significantly increased in LO2 cells after etoposide treatment (Fig. S1A). SA-β-Gal staining results showed that senescent LO2 cells were eliminated upon DMC treatment at 25 μM. Similarly, DMC + D or DMC + Q were more effective than D + Q (Fig. 1C).

We next treated non-senescent control and senescent LO2 cells with 5, 10, 25 and 50 μM DMC respectively. The results showed the viability of non-senescent cells was slightly reduced upon DMC treatment in a dose-dependent manner, and the viability of senescent cells was significantly lower than that for control cells at any concentration (Fig. 1D and S1B), suggesting DMC was a potential senolytics. Next, to investigate whether the senescent cell-clearance effect of DMC was time-dependent, we treated senescent LO2 cells with different concentrations of DMC for various durations. The results showed that DMC reduced senescent cell number in a time-dependent manner at any concentration (Fig. 1E). It was also noted that DMC treatment at 100 μM completely removed senescent cells at 48–72 h after treatment, whereas cell viabilities stabilized around 80 % and 40 % upon DMC treatment at 25 μM or 50 μM, respectively, at 48 h after treatment (Fig. 1E). We also found that DMC + D or DMC + Q were better at eliminating senescent cells than D + Q (Fig. 1F). Taken together, DMC, alone or in combination with D or Q, has a senolytic activity *in vitro*.

3.2. DMC treatment reduces senescence-associated secretory phenotype (SASP) in vitro

SASP contributes to the formation of a pro-inflammatory microenvironment around senescent cells. To explore if DMC treatment suppresses the expression of SASP factors, we treated senescent LO2 cells with DMC. We examined the mRNA levels of SASP in senescent LO2 cells after DMC treatment, and results showed that DMC treatment decreased the mRNA levels of multiple SASP factors, including *IL-1α*, *IL-1β*, *TNF-α* and *CXCL-10* (Fig. 2A–D).

Cell cycle arrest in senescent cells is prominently regulated through two main pathways: p53–Cdkn1a (p21) and/or retinoblastoma (RB)–Cdkn2a (p16) pathways [20,21]. To examine whether DMC affect the two pathways, we examined the protein levels of p21 and p16 by Western blotting. The results confirmed that the protein levels of p21 and p16 increased in senescent cells compared with non-senescent cells. The results showed that DMC treatment remarkably reduced the expression levels of p21 and p16 (Fig. 2F). In addition, we also examined the mRNA level of *p53* by qPCR. The results showed that DMC treatment reduced *p53* mRNA expression level in senescent cells (Fig. 2E). Together, these results suggest that DMC treatment reduces SASP levels and cell cycle arrest in senescent LO2 cells.

3.3. Ferrochelatase (FECH) was upregulated in senescent cells

Ferrochelatase (FECH), the key enzyme for the final step of heme biosynthesis in eukaryotes, functions to insert a Fe^{2+} ion into the center of the porphyrin ring of protoporphyrin IX (PPIX) [22]. In our previous

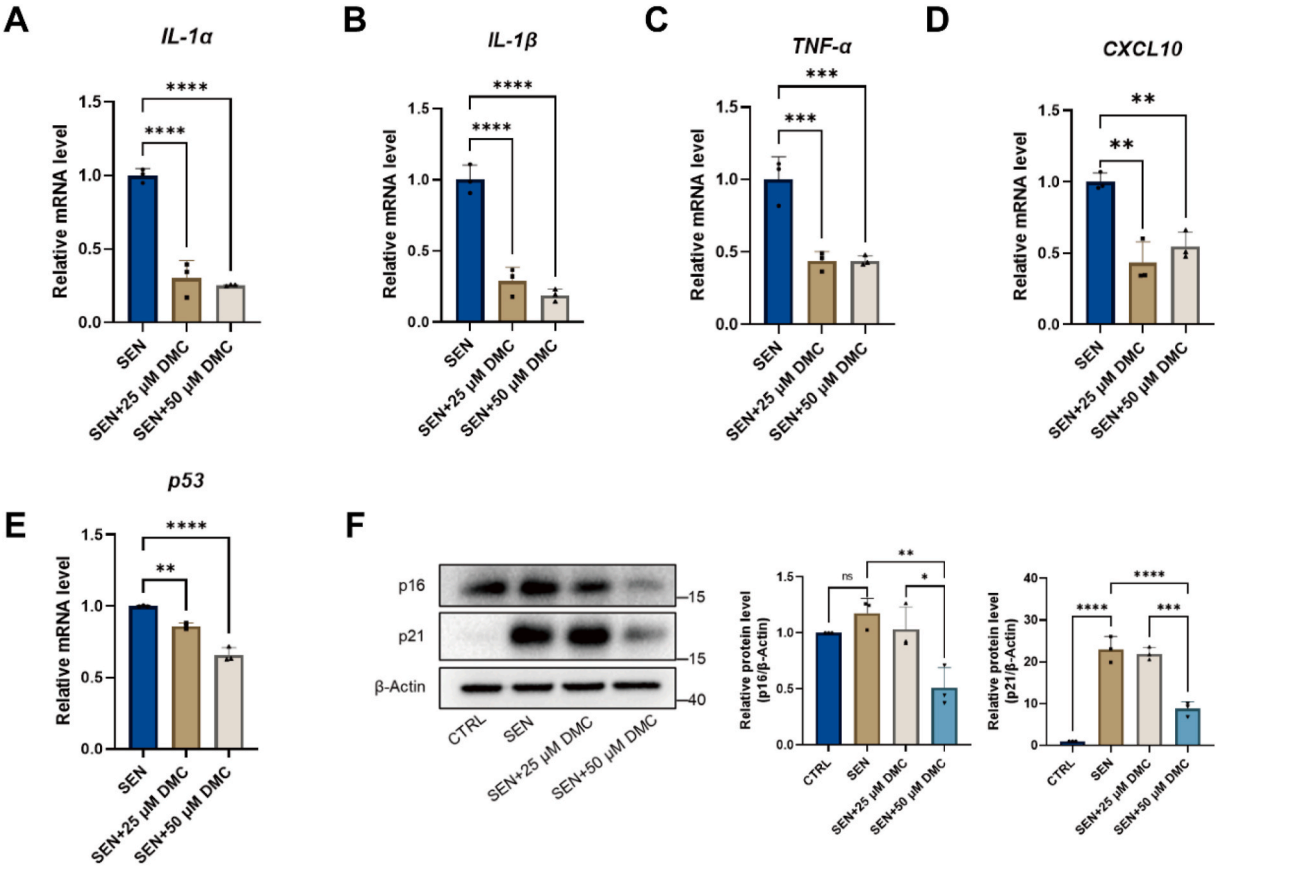

Fig. 2. DMC treatment reduces senescence-associated secretory phenotypes *in vitro*.
(A–E) Senescent LO2 cells were treated with 0, 25, 50 μM DMC for 48 h, and qPCR was used to measure mRNA levels of *IL-1α*, *IL-1β*, *TNF-α*, *CXCL-10*, and *p53* (n = 3). (F) Western blot analysis of p16 and p21 protein levels in senescent LO2 cells after DMC treatment. Graphs represent the quantification of the blots (n = 3). Ctrl: control cells. SEN: senescent cells. Data were analyzed by one-way ANOVA. ****p < 0.0001; ***p < 0.001; **p < 0.01; *p < 0.05. *p < 0.05 was considered statistically significant. All values represent the mean ± SD.

study, we demonstrated that DMC binds to FECH to inhibit its enzymatic activity [12]. To investigate if FECH is involved in cellular senescence, we performed Western blot analysis to examine the expression level of FECH in senescent LO2 and 293 T cells. The results showed that the protein level of FECH was higher in senescent cells than in non-senescent cells (Fig. 3A and B).

Next, to determine if FECH mediates DMC's effect on the clearance of senescent cells, we knocked down FECH in senescent LO2 cells using siRNA and treated the cells with DMC (Fig. 3C and D). The results showed that the cell viabilities were significantly higher in FECH knockdown (KD) than scramble negative control (NC) siRNA cells after DMC treatment at 25 μM and 50 μM (Fig. 3E). These results suggest that DMC-induced clearance of senescent cells is partially mediated by FECH. In consideration the importance of FECH in iron metabolism, by inhibiting FECH, DMC treatment may cause iron accumulation.

3.4. DMC induced ferroptosis in senescent cells

Eukaryotic cells have two primary functional forms of iron: heme and iron-sulfur clusters, and disturbed heme metabolism causes iron accumulation [23,24]. Notably, accumulated cellular iron, particularly labile ferrous iron, can react with H_2O_2 to form Fe^{3+} via Fenton reaction, which produces toxic hydroxyl radicals, thereby promoting ferroptosis [25]. DMC could bind to FECH and inhibit its enzymatic activity, which may cause iron accumulation in senescent cells. To test this hypothesis, we measured the total iron content using iron colorimetric assay, and found that the total iron content was significantly increased upon DMC treatment in a dose-dependent manner. After DMC treatment at a concentration of 50 μM, the total iron content in both senescent LO2 and 293 T cells increased approximately 3-fold (Fig. 4A–B). SsGSEA result yielded that, unlike other modes of cell death, ferroptosis was inhibited in senescent cells and instead activated after DMC treatment (Fig. 4C). It was also noted that the ferroptosis inhibitor ferrostatin-1 (Fer-1) partially reversed DMC-induced cell death (Fig. 4D and S2A). These results suggest that DMC induces iron-dependent cell death in senescent cells.

Ferroptosis is driven primarily by lipid peroxidation [25]. Malondialdehyde (MDA) is a major degradation product during lipid peroxidation that causes damage [26]. Accordingly, we performed the MDA assay, and the results showed that MDA levels significantly increased after DMC treatment in a dose-dependent manner in both senescent LO2 cells and 293 T cells (Fig. 4E–F). In addition, we also examined the expression levels of lipid peroxidation-related genes using qPCR. The results showed that the mRNA levels of lipid peroxidation-related genes, including *LPCAT3* [27], *POR* [15] and *ALOX5* [28], were all upregulated (Figs. S2B–F). Another characteristic of cells undergoing ferroptosis is reduced number of mitochondrial cristae and shrunken mitochondria [14,15]. Transmission electron microscopy (TEM) results showed that mitochondrial cristae decreased or disappeared and mitochondria became shrunken in senescent LO2 cells after DMC treatment (Fig. 4G). These results suggest that DMC treatment induces ferroptosis in senescent cells.

In addition to ferroptosis, apoptosis is another cell death process induced by senolytics in senescent cells [5,29,30]. Hence, we examined apoptosis in senescent LO2 and 293 T cells upon DMC treatment at different concentrations using Annexin V/PI staining and flow cytometry. The results showed that DMC treatment did not affect the percentages of Annexin V or PI positive cells at any tested concentration, suggesting that apoptosis was not involved in DMC-induced senescent cell death (Figs. S3A and S3B). Taken together, DMC induced ferroptosis in senescent cells.

3.5. DMC induces senescent cell ferroptosis via ferritinophagy

Ferritinophagy is a cellular process that ferritin is degraded by nuclear receptor coactivator 4 (NCOA4)-mediated autophagy [31]. Iron is

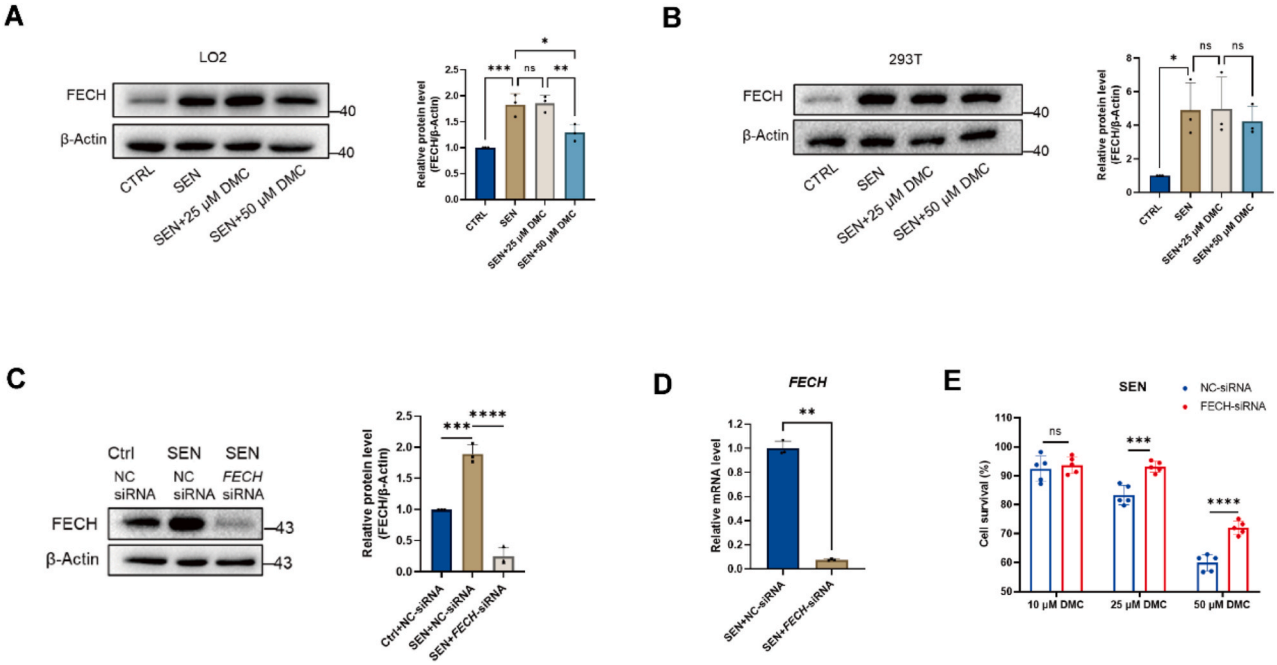

Fig. 3. FECH expression is upregulated in senescent cells.
(A–B) Western blot analysis of FECH protein levels in senescent LO2 and 293 T cells after DMC treatment. Graphs represent the quantification of the blots (n = 3). (C) Immunoblot confirmation of FECH knockdown using specific siRNAs. Graphs represent the quantification of the blots (n = 3). (D) qPCR confirmation of FECH knockdown using specific siRNAs (n = 3). (E) Cell survival assessment: Senescent *N*C-LO2 and FECH knockdown LO2 cells were treated with 10, 25, 50 μM DMC for 24 h, followed by CCK-8 analysis (n = 5). Ctrl: control cells. SEN: senescent cells. For A, B and C, data were analyzed by one-way ANOVA. For D and E, data were analyzed using Student's *t*-test. ****p < 0.0001; ***p < 0.001; **p < 0.01; *p < 0.05. *p < 0.05 was considered statistically significant. All values represent the mean ± SD.

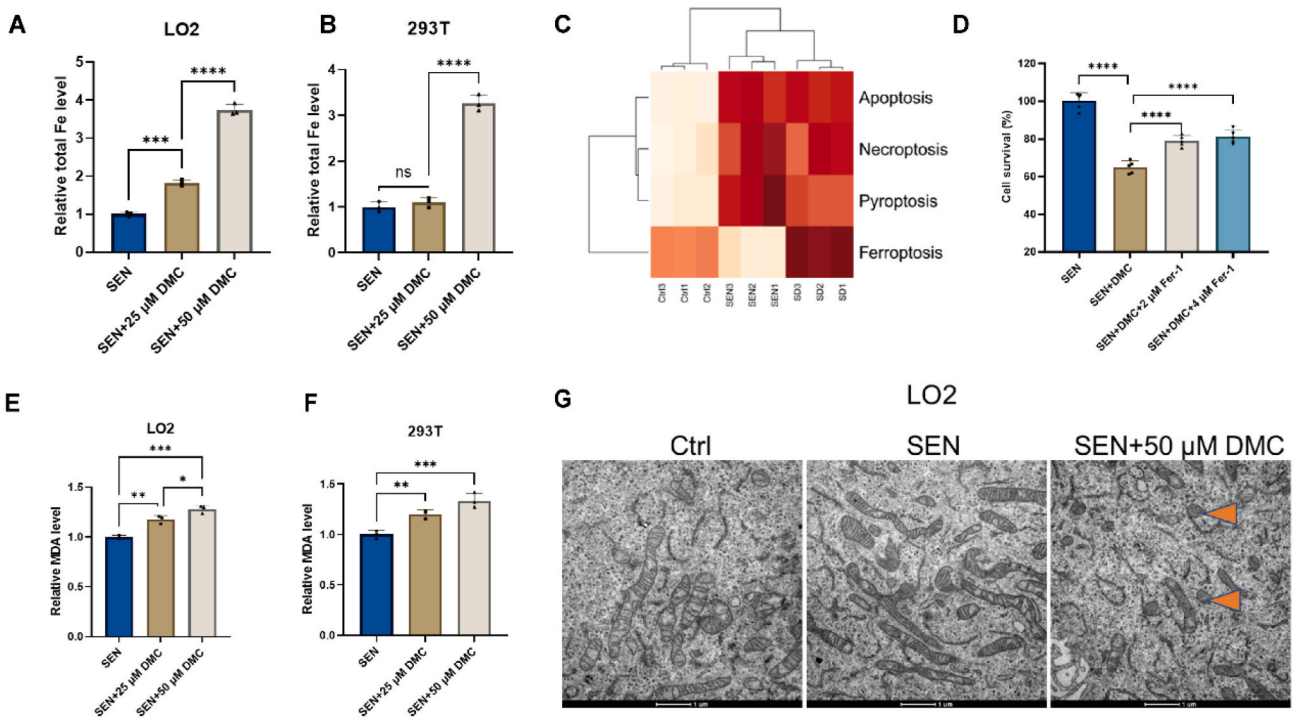

Fig. 4. DMC treatment induces ferroptosis in senescent cells.
(A–B) Senescent LO2 and 293 T cells were treated with 0, 25, 50 μM DMC for 48 h and 6 h. Total iron levels in senescent LO2 and 293 T cells were measured using an iron colorimetric assay kit (n = 3). (C) Bioinformatics analysis of TMT quantitative proteomics. The heatmap depicted the difference in activity of 4 types of cell death between the 3 groups. Ctrl, SEN, SEN + DMC (SD). (D) Cell survival assessment: Senescent LO2 cells were treated with DMSO, DMC, and Fer-1 for 24 h, followed by CCK-8 analysis (n = 5). (*E*–F) Senescent LO2 and 293 T cells were treated with 0, 25, 50 μM DMC for 48 h and 6 h. Malondialdehyde (MDA) levels in senescent LO2 and 293 T cells were measured using the MDA assay (n = 3). (G) Representative transmission electron microscopy images depicting changes in mitochondrial morphology. Scale bar: 1 μm. Ctrl: control cells. SEN: senescent cells. The differences in each inflammatory cell death pathways between the three groups were detected by the Kruskal-Wallis test and *P*-values were all <0.05. Other data were analyzed using a one-way ANOVA test. ****p < 0.0001; ***p < 0.001; **p < 0.01; *p < 0.05. *p < 0.05 was considered statistically significant. All values represent the mean ± SD.

stored in ferritin complexes under normal condition. NCOA4 binds to ferritin and mediates its delivery to the autophagosome for degradation and iron release. The protein level of ferritin in senescent cells is upregulated compared with control cells as result of the impaired ferritinophagy in senescent cell [18]. Previously, study demonstrated that DMC could induce autophagy [10]. Herein, we examine p62 and LC3 expression levels in senescent LO2 cells. The results showed that the activated form of LC3 (LC3-II) was higher in DMC treated cells, suggesting that DMC treatment induces autophagy in senescent cells (Fig. 5A and S4A). In addition, we observed that the protein and mRNA levels of NCOA4 were increased in senescent cells after DMC treatment (Fig. 5B and C). To confirm that ferritinophagy induced by DMC treatment, we first examined the protein level of ferritin by Western blot analysis. Previous study demonstrated that ferritin expression level was elevated in senescent cells [18]. Consistently, our results showed that ferritin protein levels increased in senescent LO2 and 293 T cells compared with control cells (Fig. 5D–E). The results also showed that DMC treatment decreased the protein level of ferritin in senescent cells in a dose-dependent manner (Fig. 5D–E). However, the results of qPCR analysis showed that the mRNA levels of ferritin were not changed in senescent cells after DMC treatment (Figs. S4B and S4C). Therefore, it appears that DMC treatment reduces the expression level of ferritin post-transcriptionally, likely through the degradation of ferritin protein.

In order to investigate whether ferritinophagy is involved in DMC-induced ferritin degradation, we treated senescent cells with 50 μM DMC and 100 nM Baf-A1, an autophagy inhibitor, for 24 h. The results showed that the reduction of ferritin levels was partially reversed by Baf-A1 treatment, suggesting that ferritin was degraded by ferritinophagy (Fig. 5F). Given that ferritin is the cellular iron storaging protein, its degradation likely contributed to the accumulation of free iron upon DMC treatment in senescent cells. Next, we measured the total iron content, and found that the total iron content was significantly decreased after treating senescent cells with 50 μM DMC +100 nM Baf-A1 or 25 μM chloroquine (CQ) (Fig. 5G and S4D). Taken together, these results suggest that DMC induces ferroptosis in senescent cells via ferritinophagy.

Ferroptosis was reported as inhibited in senescent cells [18]. Next, we examined the sensitivity of senescent cells upon the ferroptosis inducer RSL3 treatment. Consistent with the previous study, CCK-8 assay results showed that senescent LO2 cells had a lower cell death rate than control cells upon RSL3 treatment, suggesting that control cells were more sensitive on RSL3 (Fig. 5H). However, RSL3 and DMC co-treatment, remarkably increased cell death rate of senescent cells compared with RSL3 treatment alone (Fig. 5I), suggesting that DMC and RSL3 synergistically induces cell death in senescent cells.

3.6. *DMC treatment alleviates senescence-associated phenotypes in old mice*

Next, we sought to investigate if DMC or the combination of DMC and quercetin (DMC + Q) would eliminate senescent cells or prevent senescence-associated phenotypes *in vivo*. We recruited 20-month-old mice, and treated the mice with 50 mg/kg for DMC or 25 mg/kg for DMC +25 mg/kg for Q for 2 months (Fig. 6A). From the appearance, we observed that the hair of DMC or DMC + Q -treated mice was thicker, darker and shinier compared with non-treated control mice (Fig. 6B). In addition, through rotarod test, we observed that DMC or DMC + Q treatment increased the latency to fall from the rotarod, which suggest that the treatment improves motor coordination in old mice (Fig. 6C). To examine whether DMC or DMC + Q treatment eliminates senescent cells

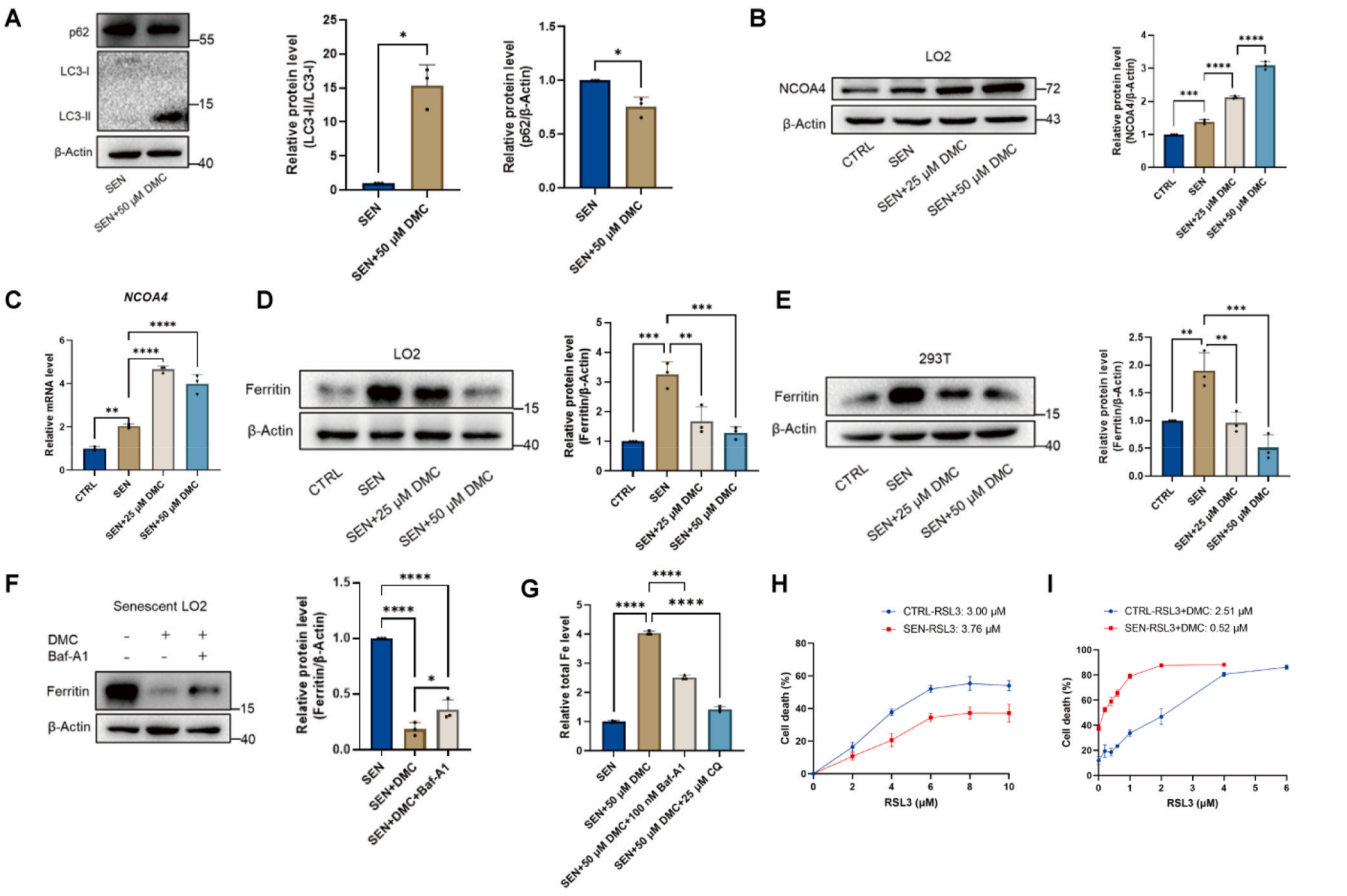

Fig. 5. DMC treatment induces ferroptosis via ferritinophagy in senescent cells.
(A) Western blot analysis of LC3 protein levels in senescent LO2 cells after treatment with 50 μM DMC for 24 h. Graphs represent the quantification of the blots (n = 3). (B) Western blot analysis of NCOA4 protein levels in senescent LO2 cells after treatment with 0, 25, 50 μM DMC for 48 h. Graphs represent the quantification of the blots (n = 3). (C) qPCR analysis of NCOA4 mRNA levels in senescent LO2 cells after treatment with 0, 25, 50 μM DMC for 48 h (n = 3). (D–E) Senescent LO2 and 293 T cells were treated with 0, 25, 50 μM DMC for 48 h and 6 h. Western blot analysis of ferritin protein levels in senescent LO2 and 293 T cells after DMC treatment. Graphs represent the quantification of the blots (n = 3). (F) Senescent LO2 cells were treated with 50 μM DMC, 50 μM DMC + 100 nM Baf-A1 for 24 h. Western blot analysis of ferritin protein levels in senescent LO2. Graphs represent the quantification of the blots (n = 3). (G) Senescent LO2 cells were treated with 50 μM DMC, 50 μM DMC + 100 nM Baf-A1, 50 μM DMC + 25 μM CQ for 24 h. Total iron levels in senescent LO2 cells were measured using an iron colorimetric assay kit (n = 3). (H) Cell death assessment: Ctrl and senescent LO2 cells were seeded in 96-well plates, treated with DMSO, RSL3 for 24 h. After treatment, CCK-8 analysis was performed, LD50 was calculated (n = 5). (I) Cell death assessment: Ctrl and senescent LO2 cells were seeded in 96-well plates, treated with DMSO, 50 μM DMC and 50 μM DMC + RSL3 for 24 h. After treatment, CCK-8 analysis was performed, LD50 was calculated (n = 4). Ctrl: control cells. SEN: senescent cells. For A, data were analyzed using Student's *t*-test. Other data were analyzed by one-way ANOVA test. ****p < 0.0001; ***p < 0.001; **p < 0.01; *p < 0.05. *p < 0.05 was considered statistically significant. All values represent the mean ± SD.

in vivo, we performed SA-β-Gal staining of liver tissues. The results showed that senescent cell number was significantly lower in mice treated with DMC or DMC + Q than control mice (Fig. 6D).

SASP secreted by senescent hepatocytes is thought to be the main mediator leading to changes in tissue homeostasis and the microenvironment [32], which led to multiple ageing-related diseases. Therefore, we next performed HE staining and immunohistochemistry (IHC) staining in liver tissues. HE staining results showed that the infiltration of immune cells in the liver was lower in DMC or DMC + Q treated mice than control mice (Fig. 6E). Results of immunohistochemistry staining showed that DMC or DMC + Q treatment decreased the SASP factors, such as IL-6 and IL-1β in liver tissues (Fig. 6E). We also examined the mRNA levels of SASP factors. In line with the IHC results, the SASP factors, including *IL-1α*, *IL-1β*, *CXCL-10*, and *MMP12*, was decreased after DMC or DMC + Q treatment (Fig. 6F). The mRNA level of F4/80, a marker of macrophages, was also reduced in the liver tissues of DMC or DMC + Q treated mice (Fig. 6F). Collectively, these results indicate that DMC or DMC + Q reduces cellular senescence and improved physiological functions in old mice.

4. Discussion

DMC is a flavonoid previously reported as a small molecule promoting longevity and health [10]. Our previous studies have shown that DMC functions as a ferroptosis inducer in cancer cells [12]. However, there were no report on the function of DMC in senescent cells. Senotherapeutics consist of senolytics and senomorphics, which selectively eliminate senescent cells and reduce SASP, respectively [30,33]. Many flavonoids are senotherapeutics, and dasatinib + quercetin is so far the most commonly used senolytics. Dasatinib is a tyrosine kinase inhibitor, which inhibits cell proliferation and migration and induces apoptosis [34]. Quercetin is a flavonoid that interacts with Bcl-2 family members to induce apoptosis [35]. In the present study, we found that DMC, DMC + dasatinib, DMC + quercetin have a characteristic of senolytics. To investigate the senolytics effects, we employed replicative senescent cells and a DNA damage-induced senescent cells model. We found that DMC and its combination with D or Q selectively eliminated senescent cells, more effectively than using D + Q alone.

Senescent cells secrete a series of pro-inflammatory cytokines,

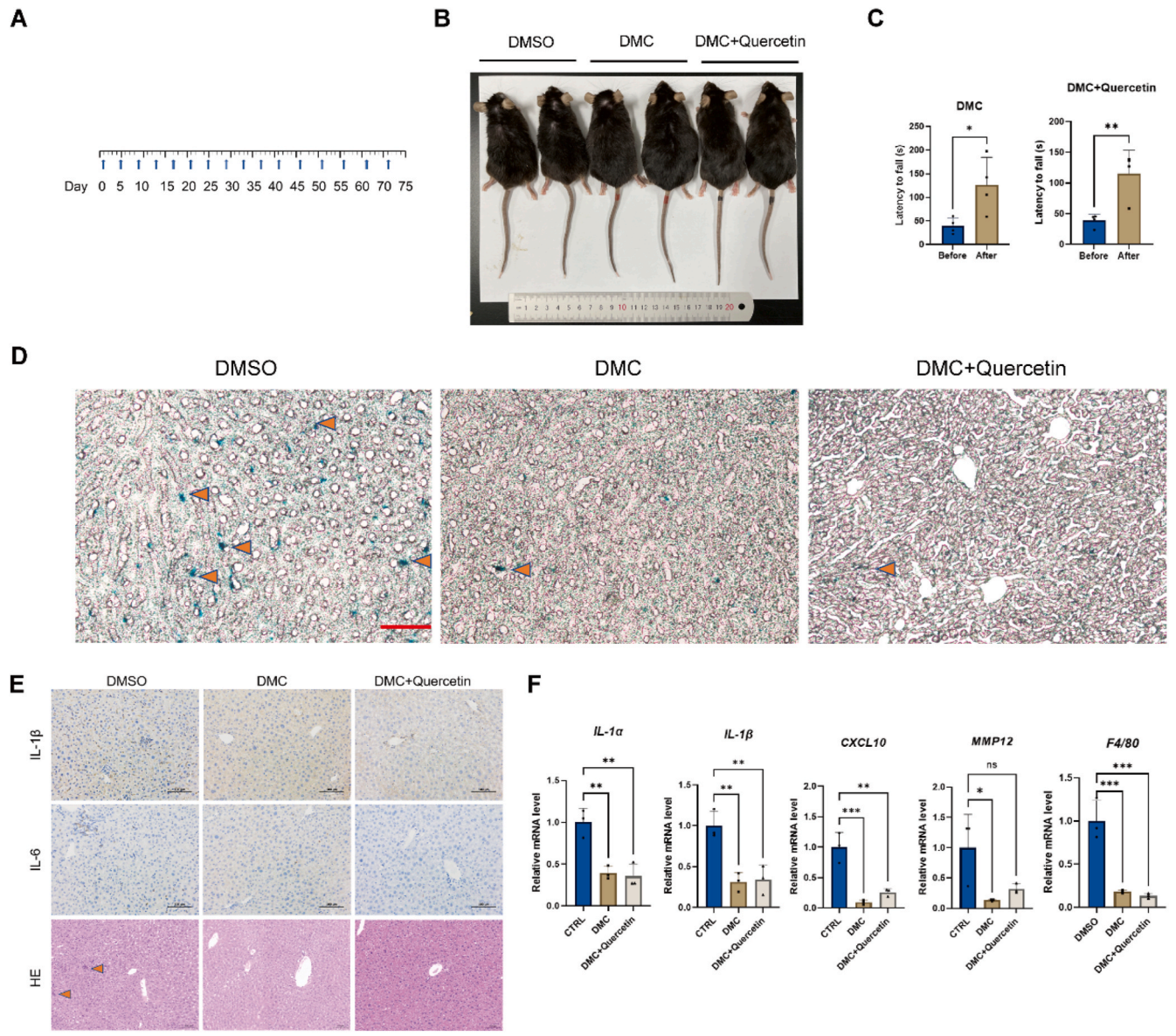

Fig. 6. DMC treatment alleviates senescence-associated phenotypes *in vivo*
(A) Flowchart of treatment. (B) Photograph of a mouse taken with a smartphone. (C) Rotarod test results (n = 4). (D) SA-β-Gal staining of liver tissues (n = 3). Scale bar: 50 μm. (E) Hematoxylin-eosin (HE) staining and immunohistochemistry staining of liver tissues. Scale bar: 100 μm. (F) qPCR analysis of mRNA levels of *IL-1α*, *IL-1β*, *CXCL-10*, *MMP12*, *F4/80* in liver tissues (n = 3). For C, data were analyzed using Student's *t*-test. Other data were analyzed by one-way ANOVA test. ****p < 0.0001; ***p < 0.001; **p < 0.01; *p < 0.05. *p < 0.05 was considered statistically significant. All values represent the mean ± SD.

chemokines, and growth factors, which is called SASP, to cause chronic inflammation and tissue dysfunction [29]. In this study, we found that DMC reduced the SASP level in senescent cells. Furthermore, senescent cells enter irreversible cell cycle arrest, which involves the activation of p53/p21 and Rb/p16. In this study we found that the expression levels of p21 and p16 were decreased after DMC treatment. The down-regulation of p21 may be attributed to the decrease of p53. In this study, we found that the mRNA level of p53 was reduced after DMC treatment.

Ferroptosis is an iron-dependent cell death process, which is accompanied by iron accumulation. Our previous study reported an important role of FECH, an enzyme inserts ferrous ion into PPIX, in ferroptosis, and showed that the inhibition of FECH by DMC led to iron accumulation in cancer cells. In this study, we found that the expression level of FECH increased in senescent cells, which may explain the sensitivity of DMC-induced ferroptosis in senescent cells.

Senescent cells are associated with impaired ferritinophagy and ferroptosis [18]. Interestingly, in our present study, we found that DMC could induce ferritinophagy, which may underlie DMC-induced ferroptosis in senescent cells. We also found that non-senescent control cells are more sensitive to RLS3-induced cell death than senescent cells. A possible reason is that the ferritin protein level was higher in senescent cells, and the binding of free ionic iron to ferritin can have a protective effect against the Fenton reaction and ferroptosis [36]. Hence, DMC-induced degradation of ferritin to the accumulation of labile iron pool and caused ferroptosis in senescent cells.

Previous study demonstrated that DMC promoted autophagy-dependent longevity in yeast, *C. elegans*, and *D. melanogaster* [10]. However, the current study suggests DMC induces ferroptosis in senescent cells. It will be interesting to examine whether DMC induced ferritinophagy in these experimental systems. More importantly, DMC has multiple targets as we described in the previous publication [11] and its effects may depend on the availability of its targets in different cells.

Inhibition of FECH that is highly expressed in senescent cells is partly responsible for senolytic effects of DMC.

In conclusion, we demonstrated that DMC caused iron overload and triggered lipid peroxidation to induce ferroptosis in senescent cells by activating ferritinophagy and inhibiting FECH activity. Moreover, we identified DMC, a natural product flavonoid, and its combination with dasatinib and quercetin as new senolytics, to alleviate senescence-associated phenotypes in old mice. Hence, DMC holds promise for treating senescence-associated diseases.

CRediT authorship contribution statement

Tianxiang Wang: Conceptualization, Data curation, Formal analysis, Investigation, Methodology, Resources, Validation, Visualization, Writing – original draft, Writing – review & editing. **Changmei Yang:** Conceptualization, Data curation, Formal analysis, Investigation, Methodology, Resources, Validation, Writing – review & editing. **Zhiqiang Li:** Investigation. **Ting Li:** Investigation. **Ran Zhang:** Writing – review & editing. **Yujiao Zhao:** Investigation. **Tianyi Cheng:** Formal analysis. **Zhaoyun Zong:** Investigation. **Yingying Ma:** Resources. **Dongyuan Zhang:** Resources. **Haiteng Deng:** Conceptualization, Funding acquisition, Methodology, Project administration, Supervision, Validation, Writing – review & editing.

Declaration of competing interest

The authors declared no competing interests.

Data availability

Data will be made available on request.

Acknowledgments

This study was supported by the National Key Research and Development Program of China (Grant No. 2021YFA1302601), the National Natural Science Foundation of China (Grant No. 82172556), and the National Natural Science Foundation of China (Grant No. T2293763).

Appendix A. Supplementary data

Supplementary data to this article can be found online at https://doi.org/10.1016/j.redox.2023.103017.

References

[1] R. Di Micco, V. Krizhanovsky, D. Baker, F. d'Adda di Fagagna, Cellular senescence in ageing: from mechanisms to therapeutic opportunities, Nat. Rev. Mol. Cell Biol. 22 (2) (2021) 75–95.
[2] B.K. Kennedy, S.L. Berger, A. Brunet, J. Campisi, A.M. Cuervo, E.S. Epel, C. Franceschi, G.J. Lithgow, R.I. Morimoto, J.E. Pessin, T.A. Rando, A. Richardson, E.E. Schadt, T. Wyss-Coray, F. Sierra, Geroscience: linking aging to chronic disease, Cell 159 (4) (2014) 709–713.
[3] J.M. van Deursen, The role of senescent cells in ageing, Nature 509 (7501) (2014) 439–446.
[4] Y. Zhu, T. Tchkonia, T. Pirtskhalava, A.C. Gower, H. Ding, N. Giorgadze, A. K. Palmer, Y. Ikeno, G.B. Hubbard, M. Lenburg, S.P. O'Hara, N.F. LaRusso, J. D. Miller, C.M. Roos, G.C. Verzosa, N.K. LeBrasseur, J.D. Wren, J.N. Farr, S. Khosla, M.B. Stout, S.J. McGowan, H. Fuhrmann-Stroissnigg, A.U. Gurkar, J. Zhao, D. Colangelo, A. Dorronsoro, Y.Y. Ling, A.S. Barghouthy, D.C. Navarro, T. Sano, P. D. Robbins, L.J. Niedernhofer, J.L. Kirkland, The Achilles' heel of senescent cells: from transcriptome to senolytic drugs, Aging Cell 14 (4) (2015) 644–658.
[5] M. Xu, T. Pirtskhalava, J.N. Farr, B.M. Weigand, A.K. Palmer, M.M. Weivoda, C. L. Inman, M.B. Ogrodnik, C.M. Hachfeld, D.G. Fraser, J.L. Onken, K.O. Johnson, G. C. Verzosa, L.G.P. Langhi, M. Weigl, N. Giorgadze, N.K. LeBrasseur, J.D. Miller, D. Jurk, R.J. Singh, D.B. Allison, K. Ejima, G.B. Hubbard, Y. Ikeno, H. Cubro, V. D. Garovic, X. Hou, S.J. Weroha, P.D. Robbins, L.J. Niedernhofer, S. Khosla, T. Tchkonia, J.L. Kirkland, Senolytics improve physical function and increase lifespan in old age, Nat. Med. 24 (8) (2018) 1246–1256.
[6] L. Zhang, L.E. Pitcher, V. Prahalad, L.J. Niedernhofer, P.D. Robbins, Recent advances in the discovery of senolytics, Mech. Ageing Dev. 200 (2021) 111587.
[7] M.M. Juca, F.M.S. Cysne Filho, J.C. de Almeida, D.D.S. Mesquita, J.R.M. Barriga, K. C.F. Dias, T.M. Barbosa, L.C. Vasconcelos, L. Leal, J.E. Ribeiro, S.M.M. Vasconcelos, Flavonoids: biological activities and therapeutic potential, Nat. Prod. Res. 34 (5) (2020) 692–705.
[8] M.J. Yousefzadeh, Y. Zhu, S.J. McGowan, L. Angelini, H. Fuhrmann-Stroissnigg, M. Xu, Y.Y. Ling, K.I. Melos, T. Pirtskhalava, C.L. Inman, C. McGuckian, E.A. Wade, J.I. Kato, D. Grassi, M. Wentworth, C.E. Burd, E.A. Arriaga, W.L. Ladiges, T. Tchkonia, J.L. Kirkland, P.D. Robbins, L.J. Niedernhofer, Fisetin is a senotherapeutic that extends health and lifespan, EBioMedicine 36 (2018) 18–28.
[9] Q. Xu, Q. Fu, Z. Li, H. Liu, Y. Wang, X. Lin, R. He, X. Zhang, Z. Ju, J. Campisi, J. L. Kirkland, Y. Sun, The flavonoid procyanidin C1 has senotherapeutic activity and increases lifespan in mice, Nat. Metab. 3 (12) (2021) 1706–1726.
[10] D. Carmona-Gutierrez, A. Zimmermann, K. Kainz, F. Pietrocola, G. Chen, S. Maglioni, A. Schiavi, J. Nah, S. Mertel, C.B. Beuschel, F. Castoldi, V. Sica, G. Trausinger, R. Raml, C. Sommer, S. Schroeder, S.J. Hofer, M.A. Bauer, T. Pendl, J. Tadic, C. Dammbrueck, Z. Hu, C. Ruckenstuhl, T. Eisenberg, S. Durand, N. Bossut, F. Aprahamian, M. Abdellatif, S. Sedej, D.P. Enot, H. Wolinski, J. Dengjel, O. Kepp, C. Magnes, F. Sinner, T.R. Pieber, J. Sadoshima, N. Ventura, S. J. Sigrist, G. Kroemer, F. Madeo, The flavonoid 4,4'-dimethoxychalcone promotes autophagy-dependent longevity across species, Nat. Commun. 10 (1) (2019) 651.
[11] C. Yang, S. Zhu, Y. Chen, Z. Liu, W. Zhang, C. Zhao, C. Luo, H. Deng, Flavonoid 4,4'-dimethoxychalcone suppresses cell proliferation via dehydrogenase inhibition and oxidative stress aggravation, Free Radic. Biol. Med. 175 (2021) 206–215.
[12] C. Yang, T. Wang, Y. Zhao, X. Meng, W. Ding, Q. Wang, C. Liu, H. Deng, Flavonoid 4,4'-dimethoxychalcone induced ferroptosis in cancer cells by synergistically activating Keap1/Nrf2/HMOX1 pathway and inhibiting FECH, Free Radic. Biol. Med. 188 (2022) 14–23.
[13] C.D. Obi, T. Bhuiyan, H.A. Dailey, A.E. Medlock, Ferrochelatase: Mapping the Intersection of iron and porphyrin metabolism in the mitochondria, Front. Cell Dev. Biol. 10 (2022) 894591.
[14] S.J. Dixon, K.M. Lemberg, M.R. Lamprecht, R. Skouta, E.M. Zaitsev, C.E. Gleason, D.N. Patel, A.J. Bauer, A.M. Cantley, W.S. Yang, B. Morrison 3rd, B.R. Stockwell, Ferroptosis: an iron-dependent form of nonapoptotic cell death, Cell 149 (5) (2012) 1060–1072.
[15] G. Lei, L. Zhuang, B. Gan, Targeting ferroptosis as a vulnerability in cancer, Nat. Rev. Cancer 22 (7) (2022) 381–396.
[16] M. Quiles Del Rey, J.D. Mancias, NCOA4-Mediated ferritinophagy: a potential Link to Neurodegeneration, Front. Neurosci. 13 (2019) 238.
[17] G.O. Latunde-Dada, Ferroptosis: role of lipid peroxidation, iron and ferritinophagy, Biochim. Biophys. Acta Gen. Subj. 1861 (8) (2017) 1893–1900.
[18] S. Masaldan, S.A.S. Clatworthy, C. Gamell, P.M. Meggyesy, A.T. Rigopoulos, S. Haupt, Y. Haupt, D. Denoyer, P.A. Adlard, A.I. Bush, M.A. Cater, Iron accumulation in senescent cells is coupled with impaired ferritinophagy and inhibition of ferroptosis, Redox Biol. 14 (2018) 100–115.
[19] X. Li, C. Li, W. Zhang, Y. Wang, P. Qian, H. Huang, Inflammation and aging: signaling pathways and intervention therapies, Signal Transduct. Targeted Ther. 8 (1) (2023).
[20] R.I. Martinez-Zamudio, L. Robinson, P.F. Roux, O. Bischof, SnapShot: cellular senescence pathways, Cell 170 (4) (2017) 816–816 e1.
[21] E. Sheekey, M. Narita, p53 in senescence - it's a marathon, not a sprint, FEBS J. 290 (5) (2023) 1212–1220.
[22] K. Sishtla, N. Lambert-Cheatham, B. Lee, D.H. Han, J. Park, S.P.B. Sardar Pasha, S. Lee, S. Kwon, A. Muniyandi, B. Park, N. Odell, S. Waller, I.Y. Park, S.J. Lee, S. Y. Seo, T.W. Corson, Small-molecule inhibitors of ferrochelatase are antiangiogenic agents, Cell Chem. Biol. 29 (6) (2022), 1010-1023 e14.
[23] H. Atamna, Heme, iron, and the mitochondrial decay of ageing, Ageing Res. Rev. 3 (3) (2004) 303–318.
[24] H. Atamna, P.B. Walter, B.N. Ames, The role of heme and iron-sulfur clusters in mitochondrial biogenesis, maintenance, and decay with age, Arch. Biochem. Biophys. 397 (2) (2002) 345–353.
[25] X. Fang, H. Ardehali, J. Min, F. Wang, The molecular and metabolic landscape of iron and ferroptosis in cardiovascular disease, Nat. Rev. Cardiol. 20 (1) (2023) 7–23.
[26] Y. Xu, K. Li, Y. Zhao, L. Zhou, Y. Liu, J. Zhao, Role of ferroptosis in Stroke, Cell. Mol. Neurobiol. 43 (1) (2023) 205–222.
[27] L. Lagrost, D. Masson, The expanding role of lyso-phosphatidylcholine acyltransferase-3 (LPCAT3), a phospholipid remodeling enzyme, in health and disease, Curr. Opin. Lipidol. 33 (3) (2022) 193–198.
[28] Q.Y. Sun, H.H. Zhou, X.Y. Mao, Emerging roles of 5-lipoxygenase Phosphorylation in inflammation and cell death, Oxid. Med. Cell. Longev. 2019 (2019) 2749173.
[29] L. Zhang, L.E. Pitcher, V. Prahalad, L.J. Niedernhofer, P.D. Robbins, Targeting cellular senescence with senotherapeutics: senolytics and senomorphics, FEBS J. 290 (5) (2023) 1362–1383.
[30] Y. Zhu, T. Tchkonia, H. Fuhrmann-Stroissnigg, H.M. Dai, Y.Y. Ling, M.B. Stout, T. Pirtskhalava, N. Giorgadze, K.O. Johnson, C.B. Giles, J.D. Wren, L. J. Niedernhofer, P.D. Robbins, J.L. Kirkland, Identification of a novel senolytic agent, navitoclax, targeting the Bcl-2 family of anti-apoptotic factors, Aging Cell 15 (3) (2016) 428–435.
[31] J.D. Mancias, X. Wang, S.P. Gygi, J.W. Harper, A.C. Kimmelman, Quantitative proteomics identifies NCOA4 as the cargo receptor mediating ferritinophagy, Nature 509 (7498) (2014) 105–109.
[32] W. Zhu, X. Zhang, M. Yu, B. Lin, C. Yu, Radiation-induced liver injury and hepatocyte senescence, Cell Death Dis. 7 (1) (2021) 244.
[33] L.J. Niedernhofer, P.D. Robbins, Senotherapeutics for healthy ageing, Nat. Rev. Drug Discov. 17 (5) (2018) 377.

[34] K. Mestermann, T. Giavridis, J. Weber, J. Rydzek, S. Frenz, T. Nerreter, A. Mades, M. Sadelain, H. Einsele, M. Hudecek, The tyrosine kinase inhibitor dasatinib acts as a pharmacologic on/off switch for CAR T cells, Sci. Transl. Med. 11 (499) (2019).

[35] G. Niu, S. Yin, S. Xie, Y. Li, D. Nie, L. Ma, X. Wang, Y. Wu, Quercetin induces apoptosis by activating caspase-3 and regulating Bcl-2 and cyclooxygenase-2 pathways in human HL-60 cells, Acta Biochim. Biophys. Sin. 43 (1) (2011) 30–37.

[36] P. Arosio, R. Ingrassia, P. Cavadini, Ferritins: a family of molecules for iron storage, antioxidation and more, Biochim. Biophys. Acta 1790 (7) (2009) 589–599.